Title: Caloric-restriction mitigates age-associated alteration in CG and non-CG methylation in the old brain.

Abbreviated title: CR mitigates DNA methylation changes in the brain

Authors: Niran Hadad[1,2,6], Archana Unnikrishnan[2,5,6], Jordan A. Jackson[2,5,6], Dustin R. Masser[2,3], Laura Otalora[2,3,5,6], David R. Stanford[2,3,6], Arlan Richardson[2,4,5,6], Willard M. Freeman[1,2,3,5,6*]

Affiliations: [1]Oklahoma Center for Neuroscience, [2]Reynolds Oklahoma Center on Aging, [3]Department of Physiology, [4]Oklahoma City VA Medical Center, [5]Department of Geriatric Medicine, [6]Oklahoma Nathan Shock Center for Aging, University of Oklahoma Health Sciences Center, Oklahoma City, OK, USA, 73104

***Corresponding Author:** Willard M. Freeman, Ph.D.; Mail: SLY-BRC 1370, 975 NE 10th St, Oklahoma City, OK 73104; Telephone: (405) 271-8000 ext. 30729; Email: wfreeman@ouhsc.edu

Conflict of interest: The authors declare no competing financial interests

Acknowledgments: The authors would like to acknowledge Laura Blanco-Berdugo for computational advice and the University of Oklahoma Supercomputing Center for Education & Research (OSCER) for allocating computational resources used for data analysis. This work was supported by the Donald W. Reynolds Foundation, the Oklahoma Center for Neuroscience translational seed grant, the Oklahoma Nathan Shock Center of Excellence in the Biology of Aging Targeted DNA Methylation and Mitochondrial Heteroplasmy Core (P30AG050911), the National Institute on Aging (R01AG045693, F31AG038285, T32AG052363), and National Eye Institute (R21EY024520, R01EY021716).

Abstract

Brain aging is marked by cognitive decline and increased susceptibility to neurodegeneration. Epigenetic mechanisms, including DNA methylation, are vital to CNS cellular function and memory formation, and are dysregulated with aging and age-related neurodegenerative disease. Caloric-restriction (CR), an established pro-longevity intervention, increases neurogenesis, improves memory function, and protects from age-associated pathologies. However, the molecular mechanisms promoting the neuroprotective effect of CR remain largely unknown. We tested the role of DNA methylation as a mechanism for CR-induced neuroprotection in the old brain. Hippocampal DNA from young (3M) and old (24M) male mice fed *ad libitum* and 24M old mice fed 40% calorie-restricted diet from 3M of age were examined by genome-wide bisulfite sequencing to measure methylation levels at base-specific resolution. Over 25 million CG and CH (non-CG) sites were examined. Of the ~40,000 differentially methylated CGs (dmCGs) and ~80,000 CHs (dmCHs) observed with aging, 35% and 38%, respectively, were prevented by CR. Unique to dmCHs, CR preferentially prevented age-related hypermethylation. A diet-specific methylation response was observed in both CG and CH contexts. CR-induced dmCHs were enriched in CG-rich regions such as promoters and CG islands including hypermethylation of DNMT1 and TET3 promoters corresponding to reduced gene expression. These findings demonstrate for the first time that caloric-restriction prevents age-induced cytosine methylation changes in the old brain in combination with CR-specific methylation changes that may function to maintain epigenetic homeostasis through epigenetic auto-regulation. The prevention of age-dmCGs/CHs by CR emphasizes the prominent role of DNA methylation as a driver of the aging process.

Significance Statement

DNA methylation is a central epigenetic regulator of genomic structure and function. Aberrant control of DNA methylation is associated with brain aging and contributes to cognitive decline and age-related

42 neurodegenerative disease. Unexplored though is whether anti-aging treatments can maintain
43 'youthful' methylation patterns in the brain. Our findings demonstrate that caloric-restriction attenuates
44 age-related changes in DNA methylation and induces changes in DNA methylation at specific sites
45 independent of aging in both neuroprotective pathways and pathways shared by different tissues
46 responsive to calorie-restriction, potentially through a combination of epigenetic auto-regulation and
47 uniquely targeted changes in methylation. These findings contribute to our understanding of the aging
48 process and the molecular mechanisms underlying anti-aging treatments.

49 **Introduction**

50 With increased life-expectancy, incidence of age-related neurodegenerative diseases such as
51 Alzheimer's, Parkinson's, and other dementias, has increased and is expected to double by 2040 (Reitz
52 et al., 2011; Reeve et al., 2014; Hickman et al., 2016). Anti-aging interventions offer promise in delaying
53 age-related impairments and neurological disease development. The most established anti-aging
54 intervention is calorie-restriction (CR), where caloric intake is reduced by 10-40%. CR consistently
55 increases lifespan and improves health span across model organisms including invertebrates (Lee et al.,
56 2006), rodents (Turturro et al., 1999), and primates (Colman et al., 2014). Several conserved
57 mechanisms have been proposed to underline the beneficial effects observed following CR including
58 inhibition of mTOR signaling (Kaeberlein et al., 2005), decreased insulin/IGF-1 signaling (Sonntag et al.,
59 1999) activation of Sirt1/Sirt2 (Bordone and Guarente, 2005) and activation of redox signaling (Hyun et
60 al., 2006), however CR is also proposed to act through cell-autonomous and tissue specific mechanisms
61 (Dacks et al., 2013; Schafer et al., 2015; Barger et al., 2017).

62 Short- and long-term CR have a protective effect against brain aging. CR increases expression of DNA
63 repair and anti-stress proteins (Kisby et al., 2010), improves glucose metabolism efficiency (Willette et
64 al., 2012b) and delays onset of inflammatory cytokines (Swindell, 2009). Specifically to the brain, CR

65 delays neurodegeneration and synaptic dysfunction (Dietrich et al., 2010; Schafer et al., 2015), improves
66 neuroendocrine function (Redman and Ravussin, 2009; Willette et al., 2012a) and promotes induction of
67 genes active in neuroprotection, neural growth (Park et al., 2013) and synaptic and neuronal function
68 (Adams et al., 2008; Fontan-Lozano et al., 2008; Schafer et al., 2015; Wood et al., 2015). At the
69 functional level, CR improves learning and memory and is beneficial in reducing anxiety and depression
70 in both rodents and humans (Inoue et al., 2004; Lutter et al., 2008; Willette et al., 2012a). CR is also
71 beneficial in alleviating pathology of age-related neurodegenerative diseases, improves cognitive
72 function (Halagappa et al., 2007) and decreases hippocampal beta-amyloid accumulation in Alzheimer's
73 models (Wang et al., 2005). Despite these positive effects on brain aging and age-related disease, the
74 molecular mechanisms underlying brain aging processes and those responsive to CR remain elusive.

75 Epigenetic modifications in the form of DNA methylation and histone modifications are proposed as
76 central regulators of the aging process (Lopez-Otin et al., 2013). DNA methylation is a malleable
77 epigenetic modification in which a methyl group is added to the 5-position of a cytosine ring and plays a
78 complex role in genomic regulation. Proper control of DNA methylation is instrumental to neural
79 differentiation, neural growth, synaptic function and intact cognitive function (Feng et al., 2010; Lister et
80 al., 2013; Grigorenko et al., 2016), key processes hampered by the aging process. Altered methylation at
81 specific genomic locations is associated with the normal aging process (Xekardaki et al., 2015; Wyss-
82 Coray, 2016). Recent studies have shown a protective epigenetic effect of anti-aging interventions in the
83 liver and kidney (Kim et al., 2016; Cole et al., 2017; Hahn et al., 2017). However, whether the response
84 by DNA methylation to aging is common between tissues or demonstrates tissue specific patterns is
85 unclear.

86 We previously described extensive age-related DNA methylation changes in the old brain (Masser et al.,
87 2017). In the current study we investigated whether these changes are prevented by CR by focusing on

88 the hippocampus, a tissue demonstrating molecular, cellular and functional impairment with old age
89 (Vanguilder and Freeman, 2011; Gray and Barnes, 2015; Seib and Martin-Villalba, 2015). Using a
90 genome-wide sequencing approach we examined the response of age-related CG and for the first time
91 CH (non-CG) methylation to CR. Additionally, we characterize unique CR-specific changes in both CG and
92 CH methylation, highlighting potential functional similarities and dissimilarities between CG and CH
93 methylation. Lastly, we show that enzymes regulating DNA methylation and demethylation are
94 suppressed by CR but not aging, in part through alteration in promoter methylation induced by CR,
95 indicating a potential mechanism for CR modulation of the neuroepigenome.

96 **Materials and methods**

97 *Animals*

98 Male C57BL/6 mice were obtained from the NIA aging and caloric restriction colony at 3 month and 24
99 month of age. Mice were housed at the University of Oklahoma Health Sciences Center animal facility
100 and maintained under SPF conditions in a HEPA barrier environment. Mice were fed irradiated NIH-31
101 mouse/rat diet (Teklad, Envigo). Both CR and AL mice were individually housed. CR was initiated at 14
102 weeks of age at 10% restriction, increased to 25% restriction at 15 weeks, and to 40% restriction at 16
103 weeks of age. Young (3 month) and old (24 month) mice were euthanized and both right and left
104 hippocampus were harvested, snap frozen in liquid nitrogen, and stored at -80°C. All animal experiments
105 were performed according to protocols approved by the OUHSC Institutional Animal Care and Use
106 Committee. Tissues from young and old *ad libitum* animals were used from a previous study (Masser et
107 al., 2017).

108 *Library preparation and sequencing*

109 Hippocampal gDNA was isolated by spin columns (Zymo duet) and genome-wide bisulfite capture
110 sequencing in accordance to previously described and validated methods (Hing et al., 2015; Masser et
111 al., 2016). gDNA was quantified by qubit (Invitrogen) and sheared by sonication (Covaris e220) to an
112 average 200bp fragment size. Fragment size was confirmed by capillary electrophoresis (DNA1000,
113 Agilent). Bisulfite sequencing library preparation was performed with 3µg DNA using SureSelect Methyl-
114 seq XT per manufacturer instructions (Agilent). In brief, sheared DNA was end-repaired, adenylated and
115 adapter ligated prior to bisulfite conversion. Libraries were sized and quantified by capillary
116 electrophoresis to ensure recovery of at least 350 ng of library. Libraries were hybridized to mouse
117 SureSelect Methyl-Seq capture library. Hybridized libraries were captured with Dynabeads MyOne
118 Streptavidin T1 magnetic beads and then bisulfite converted (EZ DNA Methylation-Gold, Zymo
119 Research), amplified according to manufacturer recommendations and purified with AMPure XP beads.
120 Following bisulfite conversion libraries were indexed and confirmed for fragment size by capillary chip
121 (DNA high sensitivity, Agilent). Prior to sequencing, libraries were quantified by PCR (KAPA library
122 quantification kit, Kapa Biosystems), diluted to 4nM, and pooled in equimolar concentrations. Pooled
123 libraries were diluted to 12 pM and then sequenced at 100 bp paired end reads on the Illumina
124 HiSeq2500 platform. Raw fastq files are available through the Sequencing Read Archive (bioproject ID
125 PRJNA397575).

126 *Informatics*

127 Paired-end reads were trimmed using CLC Genomics Workbench v10.1.1 (RRID:SCR_011853). Reads with
128 a Q-score <30 or with >1 ambiguous nucleotide were filtered. Reads passing filter were adapter trimmed
129 and an additional 3 bp were removed from the 3' and 5' ends of each read. All computational analyses
130 were performed in UNIX and R using custom scripts or published tools (where specified). Trimmed PE
131 reads were aligned as PE to the mouse GRCm38/mm10 assembly using Bismark Bisulfite Mapper version

132 0.14.4 (RRID:SCR_005604) (Krueger and Andrews, 2011). Following read mapping, methylation calling
133 was performed with Bismark methylation extractor and % methylation was determined by calculating
134 (total C methylated/total C covered) per cytosine in the genome. Only cytosines covered in all groups
135 with a cumulative coverage of 35 were used for analysis, exceeding the coverage recommendations in
136 the field for BS-seq studies (Roadmap Epigenomics et al., 2015; Ziller et al., 2015). Greater than 25M CG
137 and non-CG sites were carried forward for downstream analysis. Differential methylation between
138 groups was determined using Kruskal-Wallis H test in R, significant sites were tested for pairwise
139 multiple comparisons using Conover post hoc test using 'lsmeans', p-values were adjusted for false
140 discovery using the Benjamini-Hochberg procedure. Age-changes were defined as all differences found
141 between young-AL and old-AL animals. Diet-changes were defined as all differentially methylated
142 cytosines between Old-AL and Old-CR animals.

143 *Annotation and enrichment*

144 Coordinates for genic features including exons, introns and promoters (defined as ±1kb from TSS) were
145 downloaded from UCSC genome browser for GRCm38/mm10 reference genome. CG island shores were
146 defined as 2kb upstream and downstream from the CG island borders and shelves were defined as 2kb
147 upstream and downstream from shores. Coordinates for annotated gene regulatory regions for mouse
148 brain were downloaded from ENSEMBL open database (Zerbino et al., 2015). Over- and under-
149 representation of differentially methylated cytosines was determined by overlapping all analyzed sites
150 with the genic feature list and gene regulatory regions using 'bedtools' (Quinlan and Hall, 2010).
151 Statistical significance of over- and under- representation was determined using hypergeometric test.
152 For pathway analysis, genes were annotated for differentially methylated cytosines, only genes
153 containing >2 differentially methylated sites were included in the analysis. Analysis of pathways
154 enriched for genes affected for differential methylation was performed with the 'ReactomePA' R

155 package. Pathways with broad (>100 genes) or narrow (<7 genes) definitions were excluded.
156 Additionally, pathways with similar gene lists were consolidated. A full unedited list will be available
157 upon request.

158 *Real-Time PCR (qPCR)*

159 Expression of DNMTs (pan-DNMT1, Mm01151063_m1; E1-DNMT1, Mm00599763_m1; Alt. E1-DNMT1,
160 Mm01174085_m1; DNMT3a1, Mm00432870_m1) and TETs (TET1, Mm01169087_m1; TET2,
161 Mm00524395_m1; TET3, Mm00805756_m1) was determined by real-time qPCR as described previously
162 (Mangold et al. 2017b). β-actin (Mm02619580_g1) was used as the endogenous control and each
163 sample was analyzed in technical triplicates.

164 *Experimental Design and Statistical Analysis*

165 Genome-wide methylation analysis was performed with n=4/group. Gene expression experiments were
166 performed with n=7-8/group. All statistical analyses were performed in R. Box plots represent the 25th
167 and 75th percentiles. Differential methylation and enrichments were determined as detailed above.
168 Global methylation differences were compared using linear regression and are written as mean ± SD.
169 Analysis of gene expression using RT-qPCR was compared using One-Way ANOVA with pairwise
170 comparisons and Benjamini-Hochberg multiple testing corrections.

171 **Results**

172 *Age related CG methylation is attenuated by life-long caloric restriction*

173 To examine the effect of life-long caloric-restriction on CG methylation in the old brain, hippocampal
174 DNA was isolated from Young (3 month old, Y-AL, n=4) and old (24 month old, O-AL, n=4) male mice that
175 were fed *ad libitum* (AL) throughout life and old animals fed a 40% caloric restriction (CR) diet (24 month
176 old, O-CR, n=4) starting at 3 months of age. Using genome-wide bisulfite sequencing, base-specific

177 methylation levels across 3 million CpGs were compared between the 3 groups. Global DNA
178 methylation, i.e. the methylation averages across all analyzed CpG sites did not change with age or diet
179 (Y-AL: 42.3% ± 0.7; O-AL: 42.6% ± 0.5; O-CR: 42.6%±0.6; p=0.45 by linear regression). We defined age-
180 associated dmCGs (age-dmCGs), as any methylation difference between young-AL and old-AL animals
181 that met statistical criteria (methylation difference >|5%| and adjusted p-value < 0.05, for more details
182 see differential methylation in Methods). Comparing young-AL animals to old-AL animals, 41,586 age-
183 related age-dmCGs were identified. Examination of the methylation profile of all age-dmCGs for
184 differences between young-AL and old-CR mice reveals a pattern of regression towards that of young-
185 AL, indicating a "younger" methylation profile in age matched animals fed CR diet (Fig. 1A, B). At single
186 base resolution, life-long CR prevented 32% hypermethylated and 36% hypomethylated age-dmCGs (Fig.
187 1C). The distribution of age-dmCGs shows a higher number of hypermethylated dmCGs than
188 hypomethylated dmCGs. Prevented age-dmCGs followed a similar distribution that was proportional to
189 that observed for age-dmCGs. (Fig. 1D). Principal component analysis of age-dmCGs unaffected by CR
190 demonstrated clustering of all old animals as compared to young-AL (Fig. 1E). Parallel analysis of
191 prevented age-dmCGs separates young-AL and old-CR from old-AL on the first component, while young-
192 AL and old-CR separate on the second component (Fig. 1F). The partition of young-AL and old-CR may be
193 attributed to a subset of 416 loci that demonstrate differential methylation between Y-AL and O-CR with
194 both diet and aging, e.g. gain in methylation with age and loss in methylation with age and diet as
195 compared to Y-AL.

196 The localization of differentially methylated sites by genomic context and their interaction with other
197 epigenomic marks can aid in understanding the role of DNA methylation changes in genomic regulation.
198 Methylation changes were mapped with known coordinates of gene-centric features to annotate the
199 enrichment of differentially methylated sites. In genic features, including CG islands, shores and shelves,
200 introns, exons and promoters there was no observable difference in enrichment pattern between hyper-

201 and hypo- methylated age-dmCGs or prevented age-dmCGs (Fig. 1G). Age-dmCGs and prevented age-
202 dmCGs were enriched in introns and CGI shores while under-represented in islands, CGI shelves, exons,
203 and promoters. Depletion of age-dmCGs in promoters was more pronounced in promoters containing
204 CGI. Previous reports demonstrated that DNA methylation may alter gene expression through
205 interaction with gene regulatory regions (Roadmap Epigenomics et al., 2015). To identify enrichment at
206 specific gene regulatory regions we used the ENSEMBL brain specific regulatory build (Zerbino et al.,
207 2015) which was constructed using sequencing methods to identify CTCF binding sites, enhancers, open
208 chromatin regions, promoters, promoter flanks, and transcription factor binding sites and their specific
209 activation states (active, inactive, poised, repressed). Enrichment of age-dmCGs was predominantly
210 observed in inactive state gene regulatory regions. Inactive regions are defined as regions not associated
211 with other epigenetic marks, indicating that the effect of differential methylation at these regions is
212 independent of interaction with other known epigenetic marks. Age-dmCGs were enriched in active
213 state regulatory regions and occurred in CTCF binding sites (hypo only), enhancers (hypo and hyper),
214 open chromatin regions (hyper only), and promoter flank (hyper only). Prevented age-dmCG generally
215 demonstrated a similar enrichment pattern (Fig. 1H).

216 The interaction between gene expression and DNA methylation is still an active area of exploration. The
217 canonical view of DNA methylation regulation of gene expression through promoter or gene body
218 methylation has been challenged recently both in neurons (Sharma et al., 2016) and following CR (Hahn
219 et al., 2017). Therefore, we asked which pathways are affected by DNA methylation without
220 assumptions as to whether methylation is positively or negatively regulating a specific gene. Only genes
221 containing more than 2 dmCGs in their gene body (inclusive of promoter, introns and exons) were
222 included in this analysis. Genes were separated by those affected by hyper- and hypo- methylation.
223 Hypermethylated age-dmCGs were found in 3,266 genes and hypomethylated age-dmCGs were found in
224 1,925. Of those genes 948 were found to contain prevented hypomethylated age-dmCGs and 548

225 contained prevented hypermethylated age-dmCGs. Pathways involved in neural cell communication,
226 neural cell growth, cellular integrity, cell metabolism and inflammatory pathways were affected by both
227 hyper- and hypomethylation with aging (Fig. 1I). The Rho GTPase pathway, which is involved in neurite
228 growth and axon guidance (Hall and Lalli, 2010) and downstream of cognitive decline-related myelin
229 associated inhibitors of synaptic plasticity (Vanguilder et al., 2012) was enriched in prevented
230 hypomethylated age-dmCGs while no pathways were enriched amongst the prevented hypermethylated
231 age-dmCGs. These findings are consistent with the negative effect of aging on neuronal integrity and
232 positive cellular effect of CR on neuronal survival and growth (Seib and Martin-Villalba, 2015; Hornsby et
233 al., 2016).

234 *Age related non-CG methylation is attenuated by life-long caloric restriction*

235 The effect of calorie restriction on CH methylation has not been previously examined. CH methylation is
236 higher in the brain relative to other tissues (Lister et al., 2013), is differentially regulated as compared to
237 CG methylation in the brain (He and Ecker, 2015), and has unique functional impacts on gene regulation
238 (Lister and Mukamel, 2015). We analyzed >22M CHs sites and asked whether age-dmCHs respond
239 similarly to diet as age-dmCGs. Differential methylation of CHs was determined in a base-by-base
240 fashion, similar to CGs. The absolute methylation level of most dmCHs was generally lower than that of
241 CGs. Average global CH methylation levels did not change with age or with diet (Y-AL: 1.59% ± 0.07; O-
242 AL: 1.64% ±0.05; O-CR: 1.58%±0.8; $F_{(1,10)} = 0.61$, p=0.83 by linear regression). More dmCHs (79,058 age-
243 dmCHs) were identified to change with age compared to CGs. The methylation profile of age-dmCHs in
244 old animals fed CR diet was closer to that of young-AL animals compared to that of old animals fed *ad*
245 *libitum* (Fig. 2A). The number of hypermethylated age-dmCHs was higher than hypomethylated dmCHs
246 in a manner similar to CGs. Life-long CR prevented 59% of all hypermethylated age-dmCHs and 11% of
247 hypomethylated age-dmCHs. Prevention of hypermethylated age-dmCHs by CR was 10 times more likely

248 than diet induced preventions of hypomethylated age-dmCHs (Fig. 2B-C). Principal component analysis
249 of age-dmCHs unaffected by diet shows a distinct clustering of both AL and CR old animals compared to
250 young-AL animals (Fig. 2D). Clustering of samples by the methylation profile of prevented age-dmCHs
251 shows that old-AL animals separate from young-AL and old-CR animals (Fig. 2E).

252 Differentially methylated CHs were generally under-represented in CG islands and shelves, and in gene-
253 centric elements. The exception being an enrichment of prevented hypomethylated age-dmCH in CGI
254 shores (Fig. 2F). Taken together, under-representation of dmCHs in in CG islands and genic regions
255 indicate that changes in methylation with age, and those prevented by CR, occur primarily in intragenic
256 regions and are partially excluded from CG rich regions. Enrichment analysis of age-dmCHs in gene-
257 regulatory regions reveals that age-dmCHs and prevented age-dmCHs, regardless of gain or loss in
258 methylation, are enriched mostly in active and inactive enhancers. Hypomethylated age-dmCHs and
259 prevented age-dmCHs were also enriched in poised TF binding sites and repressed promoters (Fig. 2G).

260 Pathways enriched for genes affected by age-dmCH were functionally similar to those enriched by age-
261 dmCG, including pathways involved in metabolic regulation, cellular signaling, and regulation of neural
262 cell structure and growth. Pathways enriched for prevented age-dmCHs were primarily involved in
263 energetics, metabolism and neurite growth (Fig. 2H). Of all the pathways found to be affected by
264 differential methylation 18 were common to age-dmCHs and age-dmCGs (Fig. 2I).

265 *Gene regulatory regions are affected differentially by CR induced CG methylation*

266 Caloric-restriction was sufficient to prevent >1/3 of all age-dmCs (CGs and CHs). CR also induced DNA
267 methylation changes independent of aging as evident when comparing old-AL and old-CR animals.
268 Methylation of these CR-induced dmCGs (diet-dmCGs) is not different between young-AL and old-AL
269 animals (colored green in Fig. 3A-left scatterplot) but are differentially methylated between old-AL and
270 old-CR animals (Fig. 3A-right scatterplot). Of all differentially methylated dmCGs between old-AL and

271 old-CR, 69.4% were induced by CR and were independent of the aging process (Fig. 3B). A single base
272 example of a diet-induced change in methylation is depicted in Fig. 3C. The distribution of all diet-
273 dmCGs shows significant preference towards hypermethylation (Fig. 3D), though the average magnitude
274 of methylation change is similar between hyper- and hypo- methylation (12.3% vs -12.5%, Fig 3D).

275 The genomic localization of diet-dmCGs is different from age-dmCGs. Hypermethylated diet-dmCGs
276 were over-represented in CG islands and shores and under-represented in CG shelves. Hypomethylated
277 diet-dmCGs were only enriched in shores. With respect to genic regions diet-dmCGs were primarily
278 depleted with the exception of a small but significant over representation of hypermethylated sites in
279 exons and hypomethylated sites in introns (Fig.3E). The same distinction between hyper- and hypo- diet-
280 dmCGs was observed in gene regulatory regions. Enrichment of diet-dmCGs was primarily in poised
281 regulatory regions while enrichment of hypomethylated diet-dmCGs was observed in active regulatory
282 features, including CTCF binding sites, enhancers, open chromatin and promoter flanks. Active
283 promoters were not enriched for hyper- and hypo- methylated diet-dmCGs; however, hypermethylated
284 diet-dmCGs were enriched in inactive and repressed promoters (Fig. 3F). Genes affected by diet-dmCGs
285 were enriched for pathways involving energy regulation, inflammatory pathways and phagocytosis (Fig.
286 3G). Interestingly, we found that genes containing diet-dmCGs were enriched in DNA methylation and
287 senescence-associated secretory phenotype pathways; both pathways have been proposed as potential
288 regulators of the aging process (Lopez-Otin, 2013).

289 *Non-CG diet induced changes are clustered*

290 The diet-specific effect on methylation was also observed in non-CG sites (Fig. 4A). Changes in CH
291 methylation with diet occurred generally at lower methylation levels with the majority of changes
292 occurring under 50% (Fig. 4A – right panel), but showed no difference between young-AL and old-CR
293 (Fig. 4A – left panel). Most diet-dmCHs (75% of all differential methylation observed in CHs) were

294 independent of the aging process (Fig. 4B). Twice as many hypermethylated (64,191 sites) than
295 hypomethylated diet-dmCHs (26,237 sites) were observed, similar to diet-dmCGs. Hypermethylation of
296 diet-dmCHs was higher than hypomethylated diet-dmCHs (10% vs -8%, Fig. 4C).

297 CG dinucleotides are generally depleted from large regions of the genome but occur at specific, high
298 density regions such as in CG islands and promoters. On the other hand, the distribution of CHs is
299 relatively uniform across the genome (He and Ecker, 2015). We investigated whether age and diet
300 induced dmCHs are sporadically distributed across the genome or clustered as a result of targeted
301 changes at specific genomic loci. We computed the distance between dmCHs, 62% of all dmCHs (age
302 and diet) occurred within 10kb of one another; therefore we focused our analysis to 10kb segments. The
303 proximity of diet-dmCHs to the nearest dmCH was higher than that observed for age-dmCHs (67% diet-
304 dmCHs compared to 56% age-dmCHs, Fig. 4D). This difference was even more pronounced when
305 calculating the distance between dmCHs within 1kb (49% vs. 29%). Further examination of the clustering
306 pattern of dmCHs in 10kb and 1 kb segments revealed that the distance to the next proximal dmCH (2nd
307 dmCH, 3rd dmCH, etc.) decreased gradually for both age and diet, but more diet-dmCHs clustered
308 together between the 1st and the 6th diet-dmCHs than the 1st and 3nd age-dmCHs in 10kb segments
309 (Figure 4E). This clustering of diet-dmCHs suggests differential regulation/targeting mechanisms of CH
310 methylation in response to diet and between diet and age.

311 *Diet dmCHs are over-represented in CGI-promoters and depleted from non-CGIs promoters.*

312 Hypermethylation of diet-dmCHs was over-represented in CG islands, shores and exons, while
313 hypomethylation was over-represented in introns, a localization pattern similar to diet-dmCGs.
314 Interestingly, hypermethylated diet-dmCHs were also over-represented in promoters containing CGIs
315 but were absent from non-CGI promoters (Fig. 5A). This finding is unexpected since CH methylation is
316 often precluded from high-CG-rich regions and promoters (Lister et al., 2009; Laurent et al., 2010; Xie et

317 al., 2012; Guo et al., 2014), further supporting a regulated control of methylation by diet. Enrichment of
318 diet-dmCHs in gene regulatory regions confirms the observation of over-representation of
319 hypermethylated diet-dmCHs in promoters. Using the ENSEMBL regulatory build we further divided
320 promoters by their activation state and found that hypermethylated diet-dmCHs are enriched in active
321 and poised promoters and promoter flanks, and are under-represented in repressed and inactive
322 promoters. Enrichment of hypomethylated diet-dmCHs was mainly observed in inactive gene regulatory
323 elements (Fig. 5B).

324 Higher numbers of genes contained diet-induced CH hypermethylation (5,340 genes) than
325 hypomethylation (2,981 genes), consistent with the distribution of diet-dmCHs (Fig. 4C); however genes
326 with hypomethylated diet-dmCHs were enriched in a greater number of pathways (40 pathways by
327 hypomethylation vs 21 pathways by hypermethylation). Top enrichment pathways included those
328 regulating cell structure, neural cell communication and growth, and energy metabolism. Inflammatory
329 pathways were mostly enriched for genes containing hypomethylated dmCHs (Fig. 5C). Of the 69
330 pathways affected by both dmCHs and dmCGs we found 12 common pathways regulating inflammation
331 and neuronal integrity (Fig. 5D).

332 *Caloric restriction changes in methylation auto-regulates the DNA methylation machinery.*

333 DNA methylation regulatory enzymes (DNA methyltransferases; DNMTs and Ten-eleven Translocation;
334 TETs) mRNA and protein expression do not change in the hippocampus with aging (Hadad et al., 2016).
335 Given that diet-dmCGs were enriched in the DNA methylation pathway, we examined whether any of
336 the CR-induced changes in methylation observed in the current study mapped to DNMTs and TETs genic
337 elements. We identified 6 hypermethylated diet-dmCs (2 dmCGs and 4 dmCHs) in the promoter region
338 of TET3 (Fig. 6A), corresponding to a decrease in TET3 mRNA expression following CR (Fig. 6B). We also
339 found 9 hypermethylated diet-dmCs (6 dmCHs and 3 dmCGs) in the promoter region of DNMT1 (Fig. 6C),

340 but an examination of DNMT1 with a pan-isoform assay inclusive of all known isoforms revealed no
341 changes in expression (Fig. 6D). Promoter methylation of DNMT1 is located near two known start sites;
342 therefore we examined the expression of each isoform separately by qPCR. Expression of the exon-1
343 containing mRNAs declined significantly with diet, and minimally with aging, while the alternate exon-1
344 isoform was unchanged (Fig. 6E).

345 No other dmCs induced by CR found in our analysis were observed in the remaining DNA methylation
346 regulatory enzymes, however examination of the expression levels of these enzymes show a small but
347 significant decrease with age and diet of DNMT3a1 and a decrease in TET2 expression with diet (Fig. 3F).
348 TET1 expression did not differ with age or diet as well. These findings suggest that while DNMTs and
349 TETs are generally not regulated with age, the epigenetic effects of CR may occur through regulation of
350 DNMTs and TETs.

351 **Discussion**

352 This study examined whether DNA methylation is a neuroprotective mechanism of action of CR in
353 retarding brain aging. Given that calorie-restriction improves cognition and cellular function and that
354 altered methylation may underline age-related dysfunction in these processes, hippocampal DNA
355 methylation was quantified at base-specific resolution to identify age-associated changes in DNA
356 methylation and the effect of CR in preventing these changes, as previously reported for CG methylation
357 in the kidney and liver (Kim et al., 2016; Cole et al., 2017; Hahn et al., 2017). Our findings demonstrate
358 for the first time that base-specific prevention of age-related differential methylation by CR is observed
359 in the brain, not only in CG context but also CH. This is the first study to evaluate the effect of CR on CH
360 methylation, an observation that may be unique to neural tissues.

361 DNA methylation changes in the old hippocampus are observed in both CG and CH contexts (Masser et
362 al., 2017). These changes were enriched in inflammation related pathways, neuronal integrity, neuronal

363 function and synaptic transmission. Previous studies examining gene expression change with age in the
364 hippocampus showed enrichment in similar pathways (Keleshian et al., 2013; Stilling et al., 2014; Meng
365 et al., 2016; Mangold et al., 2017a; 2017b). Studies examining the relationship between gene expression
366 and methylation with age and CR (Hahn et al., 2017), and in the brain (Sharma et al., 2016) failed to
367 identify a simple correlation. While demonstrating causality between differential methylation of
368 thousands of sites and gene expression remains unfeasible, we hypothesize that methylation changes
369 with age contribute to the dysregulation of genes in these pathways. Based on our data, enrichment of
370 methylation changes with age commonly occurred in introns and genomic regulatory regions such as
371 open chromatin, CGI shores and CTCF binding sites and were under-represented in promoters and CG
372 islands. These findings may support a more complex role to methylation in regulating gene expression
373 during the aging process than simplistic alterations in promoters. This may also explain the discrepancies
374 between current studies and the canonical mechanisms by which methylation regulates expression.
375 Further investigation is required to discover the many intricate mechanisms by which methylation acts
376 as a genomic regulator with aging.

377 Over a third of all age-related differentially methylated cytosines were prevented by CR in age-matched
378 animals. The distribution of prevented sites in CG context was comparable to that of age-dmCGs,
379 however for CH sites CR preferentially prevented age-related hypermethylation. This may be caused by
380 the diet-specific reduction in expression of the DNA methylation regulatory enzymes, or via targeted
381 mechanisms such as recruitment of DNMTs and TETs to specific genomic locations by targeting co-
382 factors and changes to histone modifications and genome occupancy. In light of our results in which
383 both the methylation and demethylation machinery changed with diet and previous findings of altered
384 genomic regulation following CR (Chouliaras et al., 2013; Gong et al., 2015) we consider the later more
385 likely. It is worth noting that CR effects on age-related dmCs are classified as 'prevented', however the
386 possibility remains that these changes are delayed or reversed at different points throughout life. To

387 further elucidate the dynamics by which CR prevents, delays or reverses changes in DNA methylation
388 with aging, future studies examining time points across the lifespan are necessary.

389 The majority of CR-induced differentially methylated sites were independent of aging. These diet-
390 specific changes demonstrated different distributions in promoters, genes, and enhancers compared to
391 CR prevented age-related sites. Previous studies in the liver (Cole et al., 2017; Hahn et al., 2017)
392 reported enrichment of diet-induced CG hypermethylation in CG islands and gene bodies while CG
393 hypomethylation occurred in gene bodies and enhancers. Interestingly, we observed a similar
394 enrichment pattern in the brain. The commonalities in enrichment of diet-dmCGs in both liver and
395 hippocampus suggest common regulation of DNA methylation by diet across tissues that may be caused
396 by changes in regulation of common core proteins required for the targeting and recruitment of the
397 DNA methylation machinery to specific locations within the genome. Targeting of DNMTs and TETs to
398 specific genomic loci is a complex process that is not fully understood (Wu and Zhang, 2017). Post
399 translational histone modifications, have been positively and negatively correlated with DNA
400 modification (Lehnertz et al., 2003; Cedar and Bergman, 2009; Balasubramanian et al., 2012) and may be
401 altered through diet, thus changing recruitment of DNMTs and TETs. In the brain, CR attenuates age-
402 changes of DNMT3a and other epigenetic marks (Bordone and Guarente, 2005; Chouliaras et al., 2013;
403 Gong et al., 2015). Additionally, insulin signaling, specifically the PI3K/AKT pathway, a conserved
404 pathway altered by CR, was shown to modify DNA methylation through destabilization of DNMTs
405 (Popkie et al., 2010)

406 Genomic CH methylation is higher in the brain compared to other tissues (Lister et al., 2009), and has
407 been show to regulate transcription of genes involved in synaptic and neural growth (Chen et al., 2015;
408 Jang et al., 2017). Differential CH methylation has not been examined previously in the context of CR
409 and aging. Here we demonstrated that changes induced by diet in CH methylation are not sporadic and

410 are clustered at higher density than age-associated changes. Surprisingly diet-induced gain of
411 methylation at CH loci is observed in regions where CH methylation is often excluded such as promoters,
412 CG islands, TF binding sites and active enhancers (Lister et al., 2009; Laurent et al., 2010; Xie et al., 2012;
413 Guo et al., 2014). These findings provide evidence for a more controlled regulation of DNA methylation
414 following CR, potentially lost with aging. Genomic regulation of CH methylation is different than CGs but
415 remains largely unknown due to the lack of CH data from DNA methylation analyses. In the context of
416 CR, methylation of CHs appears to respond differently than CGs and serve a non-redundant role in
417 genomic regulation because 1) enrichment of dmCGs and dmCHs was different at promoters, TF binding
418 sites, enhancers and open chromatin and 2) the affinity of the DNMTs and TETs to CHs is lower than that
419 of CGs (Ramsahoye et al., 2000; Suetake et al., 2003; He and Ecker, 2015). The differential localization of
420 dmCHs as compared to dmCGs provides evidence that different, and as yet unknown, targeting
421 mechanisms are being used to regulate CH and CG methylation with diet.

422 Several pathways are known to be upregulated by food-restriction and its mimetics (Fusco and Pani,
423 2013). Prior gene expression studies in the brain have shown that mTOR signaling and insulin signaling
424 are downregulated by CR, as they are in other tissues, while brain-specific induction of pathways
425 including calcium signaling, synaptic vesicle regulation, neurotrophic signaling, neural growth,
426 differentiation and function, and neuronal integrity are also observed (Schafer et al., 2015; Wood et al.,
427 2015). We observed diet-induced methylation changes in pathways previously reported to change
428 following CR in the brain, specifically calcium signaling, energy metabolism, NGF signaling, FGFR
429 signaling, and pathways involved in axon guidance and growth. While a direct effect was not
430 established, the common findings between our study and previous gene expression studies suggest a
431 role for DNA methylation as a possible mechanism for the neuroprotective effect of CR against brain
432 aging.

433 Altered methylation patterns were also observed in DNA methylation regulatory pathways. Long-term
434 CR induced hypermethylation of both CGs and CHs in the promoters of TET3 and DNMT1, accompanied
435 by reduced expression with diet indicating a potential auto-regulation of the DNA methylation
436 machinery with diet. CR was reported to decrease TET2 and DNMT3b and increase TET3 expression in
437 the liver (Hahn et al., 2017) and decrease DNMT3a in the hippocampus (Chouliaras et al., 2011). Both
438 TET3 and DNMT1 were not previously reported to change with diet in the brain. Consistent with
439 previous results, DNMT3a1 mRNA expression decreased following CR. DNMT3a1 is considered the
440 primary enzyme for *de novo* CH methylation along with DNMT3b, however DNMT3b is expressed at low
441 levels in the brain (He and Ecker, 2015). Based on our findings of brain-specific differential expression of
442 DNMTs and TETs with CR and enrichment of differential methylation in pathways involved in neuronal
443 function, we propose that DNA methylation underlies brain-specific protective effects by CR, however
444 the targeting and recruitment of DNMTs and TETs to their genomic locations shares commonalities
445 across tissues as evident by enrichment of methylation changes at gene regulatory regions. We are the
446 first to report auto-regulation of DNA methylation by diet which appears to be specific to the brain.

447 Taken together our data supports a role of calorie-restriction in maintaining homeostasis through DNA
448 methylation. Changes in methylation were enriched in pathways shown to improve following CR and are
449 beneficial to brain aging. By including CH methylation analysis, we demonstrate similarities and
450 dissimilarities in the functions of CG and CH methylation in the protective effect induced by CR. These
451 findings highlight the importance in investigating both CG and CH methylation and propose a prominent
452 systemic role for DNA methylation in response to CR. Future studies are required in order to further
453 parse the specific mechanisms of diet-induced DNA methylation regulation and how these promote
454 brain health in old age.

455 **References**

456 Adams MM, Shi L, Linville MC, Forbes ME, Long AB, Bennett C, Newton IG, Carter CS, Sonntag WE, Riddle
457 DR, Brunso-Bechtold JK (2008) Caloric restriction and age affect synaptic proteins in
458 hippocampal CA3 and spatial learning ability. Exp Neurol 211:141-149.
459 Balasubramanian D, Akhtar-Zaidi B, Song L, Bartels CF, Veigl M, Beard L, Myeroff L, Guda K, Lutterbaugh
460 J, Willis J, Crawford GE, Markowitz SD, Scacheri PC (2012) H3K4me3 inversely correlates with
461 DNA methylation at a large class of non-CpG-island-containing start sites. Genome Med 4:47.
462 Barger JL, Vann JM, Cray NL, Pugh TD, Mastaloudis A, Hester SN, Wood SM, Newton MA, Weindruch R,
463 Prolla TA (2017) Identification of tissue-specific transcriptional markers of caloric restriction in
464 the mouse and their use to evaluate caloric restriction mimetics. Aging Cell 16:750-760.
465 Bordone L, Guarente L (2005) Calorie restriction, SIRT1 and metabolism: understanding longevity. Nat
466 Rev Mol Cell Biol 6:298-305.
467 Cedar H, Bergman Y (2009) Linking DNA methylation and histone modification: patterns and paradigms.
468 Nat Rev Genet 10:295-304.
469 Chen L, Chen K, Lavery LA, Baker SA, Shaw CA, Li W, Zoghbi HY (2015) MeCP2 binds to non-CG
470 methylated DNA as neurons mature, influencing transcription and the timing of onset for Rett
471 syndrome. Proc Natl Acad Sci U S A 112:5509-5514.
472 Chouliaras L, van den Hove DL, Kenis G, Dela Cruz J, Lemmens MA, van Os J, Steinbusch HW, Schmitz C,
473 Rutten BP (2011) Caloric restriction attenuates age-related changes of DNA methyltransferase
474 3a in mouse hippocampus. Brain Behav Immun 25:616-623.
475 Chouliaras L, van den Hove DL, Kenis G, Draanen M, Hof PR, van Os J, Steinbusch HW, Schmitz C, Rutten
476 BP (2013) Histone deacetylase 2 in the mouse hippocampus: attenuation of age-related increase
477 by caloric restriction. Curr Alzheimer Res 10:868-876.
478 Cole JJ, Robertson NA, Rather MI, Thomson JP, McBryan T, Sproul D, Wang T, Brock C, Clark W, Ideker T,
479 Meehan RR, Miller RA, Brown-Borg HM, Adams PD (2017) Diverse interventions that extend

480 mouse lifespan suppress shared age-associated epigenetic changes at critical gene regulatory
481 regions. Genome Biol 18:58.
482 Colman RJ, Beasley TM, Kemnitz JW, Johnson SC, Weindruch R, Anderson RM (2014) Caloric restriction
483 reduces age-related and all-cause mortality in rhesus monkeys. Nat Commun 5:3557.
484 Dacks PA, Moreno CL, Kim ES, Marcellino BK, Mobbs CV (2013) Role of the hypothalamus in mediating
485 protective effects of dietary restriction during aging. Front Neuroendocrinol 34:95-106.
486 Dietrich MO, Antunes C, Geliang G, Liu ZW, Borok E, Nie Y, Xu AW, Souza DO, Gao Q, Diano S, Gao XB,
487 Horvath TL (2010) Agrp neurons mediate Sirt1's action on the melanocortin system and energy
488 balance: roles for Sirt1 in neuronal firing and synaptic plasticity. J Neurosci 30:11815-11825.
489 Feng J, Zhou Y, Campbell SL, Le T, Li E, Sweatt JD, Silva AJ, Fan G (2010) DNMT1 and DNMT3a maintain
490 DNA methylation and regulate synaptic function in adult forebrain neurons. Nat Neurosci
491 13:423-430.
492 Fontan-Lozano A, Lopez-Lluch G, Delgado-Garcia JM, Navas P, Carrion AM (2008) Molecular bases of
493 caloric restriction regulation of neuronal synaptic plasticity. Mol Neurobiol 38:167-177.
494 Fusco S, Pani G (2013) Brain response to calorie restriction. Cell Mol Life Sci 70:3157-3170.
495 Gong H, Qian H, Ertl R, Astle CM, Wang GG, Harrison DE, Xu X (2015) Histone modifications change with
496 age, dietary restriction and rapamycin treatment in mouse brain. Oncotarget 6:15882-15890.
497 Gray DT, Barnes CA (2015) Distinguishing adaptive plasticity from vulnerability in the aging
498 hippocampus. Neuroscience 309:17-28.
499 Grigorenko EL, Kornilov SA, Naumova OY (2016) Epigenetic regulation of cognition: A circumscribed
500 review of the field. Dev Psychopathol 28:1285-1304.
501 Guo JU, Su Y, Shin JH, Shin J, Li H, Xie B, Zhong C, Hu S, Le T, Fan G, Zhu H, Chang Q, Gao Y, Ming GL, Song
502 H (2014) Distribution, recognition and regulation of non-CpG methylation in the adult
503 mammalian brain. Nat Neurosci 17:215-222.

504 Hadad N, Masser DR, Logan S, Wronowski B, Mangold CA, Clark N, Otalora L, Unnikrishnan A, Ford MM,
505 Giles CB, Wren JD, Richardson A, Sonntag WE, Stanford DR, Freeman W (2016) Absence of
506 genomic hypomethylation or regulation of cytosine-modifying enzymes with aging in male and
507 female mice. Epigenetics Chromatin 9:30.
508 Hahn O, Gronke S, Stubbs TM, Ficz G, Hendrich O, Krueger F, Andrews S, Zhang Q, Wakelam MJ, Beyer A,
509 Reik W, Partridge L (2017) Dietary restriction protects from age-associated DNA methylation and
510 induces epigenetic reprogramming of lipid metabolism. Genome Biol 18:56.
511 Halagappa VK, Guo Z, Pearson M, Matsuoka Y, Cutler RG, Laferla FM, Mattson MP (2007) Intermittent
512 fasting and caloric restriction ameliorate age-related behavioral deficits in the triple-transgenic
513 mouse model of Alzheimer's disease. Neurobiol Dis 26:212-220.
514 Hall A, Lalli G (2010) Rho and Ras GTPases in axon growth, guidance, and branching. Cold Spring Harb
515 Perspect Biol 2:a001818.
516 He Y, Ecker JR (2015) Non-CG Methylation in the Human Genome. Annu Rev Genomics Hum Genet
517 16:55-77.
518 Hickman RA, Faustin A, Wisniewski T (2016) Alzheimer Disease and Its Growing Epidemic: Risk Factors,
519 Biomarkers, and the Urgent Need for Therapeutics. Neurol Clin 34:941-953.
520 Hing B, Ramos E, Braun P, McKane M, Jancic D, Tamashiro KL, Lee RS, Michaelson JJ, Druley TE, Potash JB
521 (2015) Adaptation of the targeted capture Methyl-Seq platform for the mouse genome
522 identifies novel tissue-specific DNA methylation patterns of genes involved in
523 neurodevelopment. Epigenetics 10:581-596.
524 Hornsby AK, Redhead YT, Rees DJ, Ratcliff MS, Reichenbach A, Wells T, Francis L, Amstalden K, Andrews
525 ZB, Davies JS (2016) Short-term calorie restriction enhances adult hippocampal neurogenesis
526 and remote fear memory in a Ghsr-dependent manner. Psychoneuroendocrinology 63:198-207.

527 Hyun DH, Emerson SS, Jo DG, Mattson MP, de Cabo R (2006) Calorie restriction up-regulates the plasma
528 membrane redox system in brain cells and suppresses oxidative stress during aging. Proc Natl
529 Acad Sci U S A 103:19908-19912.
530 Inoue K, Zorrilla EP, Tabarin A, Valdez GR, Iwasaki S, Kiriike N, Koob GF (2004) Reduction of anxiety after
531 restricted feeding in the rat: implication for eating disorders. Biol Psychiatry 55:1075-1081.
532 Jang HS, Shin WJ, Lee JE, Do JT (2017) CpG and Non-CpG Methylation in Epigenetic Gene Regulation and
533 Brain Function. Genes (Basel) 8.
534 Kaeberlein M, Powers RW, 3rd, Steffen KK, Westman EA, Hu D, Dang N, Kerr EO, Kirkland KT, Fields S,
535 Kennedy BK (2005) Regulation of yeast replicative life span by TOR and Sch9 in response to
536 nutrients. Science 310:1193-1196.
537 Keleshian VL, Modi HR, Rapoport SI, Rao JS (2013) Aging is associated with altered inflammatory,
538 arachidonic acid cascade, and synaptic markers, influenced by epigenetic modifications, in the
539 human frontal cortex. J Neurochem 125:63-73.
540 Kim CH, Lee EK, Choi YJ, An HJ, Jeong HO, Park D, Kim BC, Yu BP, Bhak J, Chung HY (2016) Short-term
541 calorie restriction ameliorates genomewide, age-related alterations in DNA methylation. Aging
542 Cell.
543 Kisby GE, Kohama SG, Olivas A, Churchwell M, Doerge D, Spangler E, de Cabo R, Ingram DK, Imhof B, Bao
544 G, Kow YW (2010) Effect of caloric restriction on base-excision repair (BER) in the aging rat brain.
545 Exp Gerontol 45:208-216.
546 Krueger F, Andrews SR (2011) Bismark: a flexible aligner and methylation caller for Bisulfite-Seq
547 applications. Bioinformatics 27:1571-1572.
548 Laurent L, Wong E, Li G, Huynh T, Tsirigos A, Ong CT, Low HM, Kin Sung KW, Rigoutsos I, Loring J, Wei CL
549 (2010) Dynamic changes in the human methylome during differentiation. Genome Res 20:320-
550 331.

551 Lee GD, Wilson MA, Zhu M, Wolkow CA, de Cabo R, Ingram DK, Zou S (2006) Dietary deprivation extends
552 lifespan in Caenorhabditis elegans. Aging Cell 5:515-524.
553 Lehnertz B, Ueda Y, Derijck AA, Braunschweig U, Perez-Burgos L, Kubicek S, Chen T, Li E, Jenuwein T,
554 Peters AH (2003) Suv39h-mediated histone H3 lysine 9 methylation directs DNA methylation to
555 major satellite repeats at pericentric heterochromatin. Curr Biol 13:1192-1200.
556 Lister R, Mukamel EA (2015) Turning over DNA methylation in the mind. Front Neurosci 9:252.
557 Lister R, Pelizzola M, Dowen RH, Hawkins RD, Hon G, Tonti-Filippini J, Nery JR, Lee L, Ye Z, Ngo QM,
558 Edsall L, Antosiewicz-Bourget J, Stewart R, Ruotti V, Millar AH, Thomson JA, Ren B, Ecker JR
559 (2009) Human DNA methylomes at base resolution show widespread epigenomic differences.
560 Nature 462:315-322.
561 Lister R et al. (2013) Global epigenomic reconfiguration during mammalian brain development. Science
562 341:1237905.
563 Lopez-Otin C, Blasco MA, Partridge L, Serrano M, Kroemer G (2013) The hallmarks of aging. Cell
564 153:1194-1217.
565 Lutter M, Krishnan V, Russo SJ, Jung S, McClung CA, Nestler EJ (2008) Orexin signaling mediates the
566 antidepressant-like effect of calorie restriction. J Neurosci 28:3071-3075.
567 Mangold CA, Wronowski B, Du M, Masser DR, Hadad N, Bixler GV, Brucklacher RM, Ford MM, Sonntag
568 WE, Freeman WM (2017a) Sexually divergent induction of microglial-associated
569 neuroinflammation with hippocampal aging. J Neuroinflammation 14:141.
570 Mangold CA, Masser DR, Stanford DR, Bixler GV, Pisupati A, Giles CB, Wren JD, Ford MM, Sonntag WE,
571 Freeman WM (2017b) CNS-wide Sexually Dimorphic Induction of the Major Histocompatibility
572 Complex 1 Pathway With Aging. J Gerontol A Biol Sci Med Sci 72:16-29.

573 Masser DR, Hadad N, Porter H, Mangold CA, Unnikrishnan A, Ford MM, Giles CB, Georgescu C,
574 Dozmorov MG, Wren JD, Richardson A, Stanford DR, Freeman WM (2017) Sexually divergent
575 DNA methylation patterns with brain aging. Aging Cell *in press.*
576 Masser DR, Stanford DR, Hadad N, Giles CB, Wren JD, Sonntag WE, Richardson A, Freeman WM (2016)
577 Bisulfite oligonucleotide-capture sequencing for targeted base- and strand-specific absolute 5-
578 methylcytosine quantitation. Age (Dordr) 38:49.
579 Meng G, Zhong X, Mei H (2016) A Systematic Investigation into Aging Related Genes in Brain and Their
580 Relationship with Alzheimer's Disease. PLoS One 11:e0150624.
581 Park JH, Glass Z, Sayed K, Michurina TV, Lazutkin A, Mineyeva O, Velmeshev D, Ward WF, Richardson A,
582 Enikolopov G (2013) Calorie restriction alleviates the age-related decrease in neural progenitor
583 cell division in the aging brain. Eur J Neurosci 37:1987-1993.
584 Popkie AP, Zeidner LC, Albrecht AM, D'Ippolito A, Eckardt S, Newsom DE, Groden J, Doble BW, Aronow
585 B, McLaughlin KJ, White P, Phiel CJ (2010) Phosphatidylinositol 3-kinase (PI3K) signaling via
586 glycogen synthase kinase-3 (Gsk-3) regulates DNA methylation of imprinted loci. J Biol Chem
587 285:41337-41347.
588 Quinlan AR, Hall IM (2010) BEDTools: a flexible suite of utilities for comparing genomic features.
589 Bioinformatics 26:841-842.
590 Ramsahoye BH, Biniszkiewicz D, Lyko F, Clark V, Bird AP, Jaenisch R (2000) Non-CpG methylation is
591 prevalent in embryonic stem cells and may be mediated by DNA methyltransferase 3a. Proc Natl
592 Acad Sci U S A 97:5237-5242.
593 Redman LM, Ravussin E (2009) Endocrine alterations in response to calorie restriction in humans. Mol
594 Cell Endocrinol 299:129-136.
595 Reeve A, Simcox E, Turnbull D (2014) Ageing and Parkinson's disease: why is advancing age the biggest
596 risk factor? Ageing Res Rev 14:19-30.

597 Reitz C, Brayne C, Mayeux R (2011) Epidemiology of Alzheimer disease. Nat Rev Neurol 7:137-152.
598 Roadmap Epigenomics C et al. (2015) Integrative analysis of 111 reference human epigenomes. Nature
599 518:317-330.
600 Schafer MJ, Dolgalev I, Alldred MJ, Heguy A, Ginsberg SD (2015) Calorie Restriction Suppresses Age-
601 Dependent Hippocampal Transcriptional Signatures. PLoS One 10:e0133923.
602 Seib DR, Martin-Villalba A (2015) Neurogenesis in the Normal Ageing Hippocampus: A Mini-Review.
603 Gerontology 61:327-335.
604 Sharma A, Klein SS, Barboza L, Lohdi N, Toth M (2016) Principles Governing DNA Methylation during
605 Neuronal Lineage and Subtype Specification. J Neurosci 36:1711-1722.
606 Sonntag WE, Lynch CD, Cefalu WT, Ingram RL, Bennett SA, Thornton PL, Khan AS (1999) Pleiotropic
607 effects of growth hormone and insulin-like growth factor (IGF)-1 on biological aging: inferences
608 from moderate caloric-restricted animals. J Gerontol A Biol Sci Med Sci 54:B521-538.
609 Stilling RM, Benito E, Gertig M, Barth J, Capece V, Burkhardt S, Bonn S, Fischer A (2014) De-regulation of
610 gene expression and alternative splicing affects distinct cellular pathways in the aging
611 hippocampus. Front Cell Neurosci 8:373.
612 Suetake I, Miyazaki J, Murakami C, Takeshima H, Tajima S (2003) Distinct enzymatic properties of
613 recombinant mouse DNA methyltransferases DNMT3a and DNMT3b. J Biochem 133:737-744.
614 Swindell WR (2009) Genes and gene expression modules associated with caloric restriction and aging in
615 the laboratory mouse. BMC Genomics 10:585.
616 Turturro A, Witt WW, Lewis S, Hass BS, Lipman RD, Hart RW (1999) Growth curves and survival
617 characteristics of the animals used in the Biomarkers of Aging Program. J Gerontol A Biol Sci
618 Med Sci 54:B492-501.
619 Vanguilder HD, Freeman WM (2011) The hippocampal neuroproteome with aging and cognitive decline:
620 past progress and future directions. Front Aging Neurosci 3:8.

621 Vanguilder HD, Bixler GV, Sonntag WE, Freeman WM (2012) Hippocampal expression of myelin-
622 associated inhibitors is induced with age-related cognitive decline and correlates with deficits of
623 spatial learning and memory. J Neurochem 121:77-98.
624 Wang J, Ho L, Qin W, Rocher AB, Seror I, Humala N, Maniar K, Dolios G, Wang R, Hof PR, Pasinetti GM
625 (2005) Caloric restriction attenuates beta-amyloid neuropathology in a mouse model of
626 Alzheimer's disease. FASEB J 19:659-661.
627 Willette AA, Coe CL, Colman RJ, Bendlin BB, Kastman EK, Field AS, Alexander AL, Allison DB, Weindruch
628 RH, Johnson SC (2012a) Calorie restriction reduces psychological stress reactivity and its
629 association with brain volume and microstructure in aged rhesus monkeys.
630 Psychoneuroendocrinology 37:903-916.
631 Willette AA, Bendlin BB, Colman RJ, Kastman EK, Field AS, Alexander AL, Sridharan A, Allison DB,
632 Anderson R, Voytko ML, Kemnitz JW, Weindruch RH, Johnson SC (2012b) Calorie restriction
633 reduces the influence of glucoregulatory dysfunction on regional brain volume in aged rhesus
634 monkeys. Diabetes 61:1036-1042.
635 Wood SH, van Dam S, Craig T, Tacutu R, O'Toole A, Merry BJ, de Magalhaes JP (2015) Transcriptome
636 analysis in calorie-restricted rats implicates epigenetic and post-translational mechanisms in
637 neuroprotection and aging. Genome Biol 16:285.
638 Wu X, Zhang Y (2017) TET-mediated active DNA demethylation: mechanism, function and beyond. Nat
639 Rev Genet.
640 Wyss-Coray T (2016) Ageing, neurodegeneration and brain rejuvenation. Nature 539:180-186.
641 Xekardaki A, Kovari E, Gold G, Papadimitropoulou A, Giacobini E, Herrmann F, Giannakopoulos P, Bouras
642 C (2015) Neuropathological changes in aging brain. Adv Exp Med Biol 821:11-17.

643 Xie W, Barr CL, Kim A, Yue F, Lee AY, Eubanks J, Dempster EL, Ren B (2012) Base-resolution analyses of
644 sequence and parent-of-origin dependent DNA methylation in the mouse genome. Cell 148:816-
645 831.
646 Zerbino DR, Wilder SP, Johnson N, Juettemann T, Flicek PR (2015) The ensembl regulatory build.
647 Genome Biol 16:56.
648 Ziller MJ, Hansen KD, Meissner A, Aryee MJ (2015) Coverage recommendations for methylation analysis
649 by whole-genome bisulfite sequencing. Nat Methods 12:230-232

650

651 **Figure Legends**

652 **Figure 1**: Caloric-restriction prevents age-associated differential CG methylation. **A.** Scatterplot depicting
653 significant age-dmCG (n = 41,586, adjusted p-value < 0.05 & methylation difference between Old-AL and
654 Young-AL > |5%|, Kruskal-Wallis H test with Conover pairwise comparisons followed by false-discovery
655 rate multiple testing corrections) methylation levels between young *ad libitum* (Y-AL) and old *ad libitum*
656 (O-AL) groups (red dots) and young *ad libitum* (Y-AL) and old calorie-restricted (O-CR) groups (blue dots).
657 Linear regression lines pass through Y-AL ~ Y-AL (black), O-AL ~ Y-AL (blue) and O-CR ~ Y-AL (dotted
658 green) age-dmCG methylation values separated by hyper- and hypo- age-dmCGs. Calorie-restriction diet
659 causes a 'younger' methylation profile in age-associated differentially methylated sites. **B.** Single base
660 representatives of an age-dmCG (left) and a prevented age-dmCG (right). **C.** Quantification of the
661 number of age-dmCGs by hypermethylation (blue) and hypomethylation (red) in animals fed *ad libitum*
662 (AL) or calorie-restricted (CR) diet. Grey indicates age-dmCGs prevented by caloric-restriction
663 (n=13,950). **D.** Distribution plot of age-dmCGs (red) and prevented age-dmCGs (blue). Age-dmCGs and
664 those prevented by CR follow a similar distribution. **E, F.** PCA plots of age-dmCGs **(E)** and prevented age-
665 dmCGs (**F**) showing clustering of old animals in age-dmCGs but separation in prevented age-dmCGs. **G.**

666 Enrichment of age-dmCGs and prevented age-dmCGs in gene-centric regions, only significant
667 enrichments are shown ($p < 0.05$, hypergeometric test). **H.** Enrichment of age-dmCGs and prevented
668 age-dmCGs in gene-regulatory regions. Red indicates under-representation (log(odds ratio) < 0 & p-
669 value < 0.05, hypergeometric test), blue indicates over-representation (log(odds ratio) > 0 & p-value <
670 0.05, hypergeometric test) and white shows no significance (p-value > 0.05). **I.** Pathway analysis of genes
671 containing significant age-dmCGs or prevented age-dmCGs. Top enrichment pathways are shown (FDR
672 adjusted p-values < 0.01). Circle size indicates the ratio of genes containing age-dmCGs or prevented
673 age-dmCGs in a pathway, color indicates p-values. No pathways were enriched for genes containing >2
674 prevented hypomethylated age-dmCGs.

675 **Figure 2:** Caloric-restriction prevents age-associated differential CH methylation. **A.** Scatterplot depicting
676 significant age-dmCH (n = 79,056, adjusted $p < 0.05$ & methylation difference between Old-AL and
677 Young-AL > |5%|, Kruskal-Wallis H test with Conover pairwise comparisons followed by false-discovery
678 rate multiple testing corrections) methylation levels between young *ad libitum* (Y-AL) and old *ad libitum*
679 (O-AL) groups (red dots) and young *ad lib* (Y-AL) and old calorie-restricted (O-CR) groups (blue dots).
680 Linear regression lines pass through Y-AL ~ Y-AL (black), O-AL ~ Y-AL (blue) and O-CR ~ Y-AL (dotted
681 green) age-dmCH methylation values separated by hyper- and hypo- age-dmCHs. **B.** Quantification of
682 the number of age-dmCHs by hypermethylation (blue) and hypomethylation (red) in animals fed *ad*
683 *libitum* (AL) or calorie-restricted (CR) diet. Grey indicates age-dmCHs prevented by caloric-restriction (n
684 = 29,880). **C.** Distribution plot of age-dmCHs (red) and prevented age-dmCHs (blue). The probability of
685 hypermethylated age-dmCH to be prevented by diet was higher than that of hypomethylated age-dmCH
686 (0.59 prevented hyper compared to 0.11 prevented hypos). **D, E.** PCA plots of age-dmCHs (**D**) and
687 prevented age-dmCHs (**E**). **F.** Enrichment of age-dmCHs and prevented age-dmCHs in gene-centric
688 regions, only significant enrichments are shown ($p < 0.05$, hypergeometric test). **G.** Enrichment of age-
689 dmCHs and prevented age-dmCHs in gene-regulatory regions. Red indicates under-representation (log

690 (odds ratio) < 0 & p-value < 0.05, hypergeometric test), blue indicates over-representation (log(odds
691 ratio) > 0 & p-value < 0.05, hypergeometric test) and white blocks did not reach statistical significance **H.**
692 Pathway analysis of genes containing significant age-dmCHs or prevented age-dmCHs. Top enrichment
693 pathways are shown (FDR adjusted p-values < 0.01). Circle size indicates the ratio of genes containing >2
694 age-dmCHs or prevented age-dmCHs in a pathway, color indicates p-values. I. Overlap between
695 pathways enriched for age-dmCHs and age-dmCGs.

696 **Figure 3:** CR induces changes in CG methylation independent of aging. **A.** *Left*: 3D scatterplot showing
697 the methylation levels of significant diet-dmCGs including unique diet-dmCGs (green) and age-dmCGs
698 prevented by CR (blue) (adjusted p < 0.05 & methylation difference between Old-AL and Old-CR > |5%|,
699 Kruskal-Wallis H test with Conover pairwise comparisons followed by false-discovery rate multiple
700 testing corrections) focusing on young-AL and old-AL. *Right*: 90° rotation on the Y-axis of the 3D plot
701 showing that unique diet-dmCGs (green) regress away from the midline when comparing old-AL and
702 Old-CR methylation levels. **B.** Proportion of diet-dmCGs unique to CR (green) and those with an age
703 interaction (prevented age-dmCGs, blue) (N = 46,052). **C.** Single base example of a unique diet-dmCG. **D.**
704 Distribution of diet-dmCGs. Dotted lines mark the average methylation differences of hypomethylated
705 diet-dmCGs (red, -12.5%) and hypermethylated diet-dmCGs (green, 12.3%). **E.** Enrichment of diet-
706 dmCGs in gene-centric regions (p < 0.05, hypergeometric test). **F.** Enrichment of diet-dmCGs in gene-
707 regulatory regions. Red indicates under-representation (log odds ratio < 0 & p-value < 0.05,
708 hypergeometric test), blue indicates over-representation (log odds ratio > 0 & p-value < 0.05,
709 hypergeometric test) and white show no significance **G.** Pathway analysis of genes containing >2
710 significant diet-dmCGs. Top enrichment pathways are shown (FDR adjusted p-values < 0.01). Circle size
711 indicates the ratio of genes containing diet-dmCGs in a pathway, color indicates p-values.

712 **Figure 4:** CR induced differential CH methylation is clustered at specific genomic loci**.** A. *Left*: 3D
713 scatterplot showing the methylation levels of significant diet-dmCHs including unique diet-dmCHs
714 (green) and age-dmCHs prevented by diet (blue) (adjusted $p < 0.05$ & methylation difference between
715 Old-AL and Old-CR > |5%|, Kruskal-Wallis H test with Conover pairwise comparisons followed by false-
716 discovery rate multiple testing corrections) focusing on young-AL and old-AL. *Right*: 90° rotation on the
717 Y-axis of the 3D plot showing unique diet-dmCH (green) regress away from the midline when comparing
718 old-AL and Old-CR methylation levels. **B.** Proportion of diet-dmCHs unique to CR (green) and those with
719 age interaction (prevented age-dmCHs, blue) (N = 90,428). **C.** Distribution of diet-dmCHs. Dotted lines
720 mark the average methylation differences of hypomethylated diet-dmCHs (red, 8%) and
721 hypermethylated diet-dmCHs (green, 10%). **D.** Distribution plot comparing the proximity between
722 dmCHs by age and diet focusing on 10 kb segments. **E.** Line graph representing % of dmCHs by degree of
723 proximity within 10kb (solid lines) or 1kb (dotted line) by age or by diet.

724 **Figure 5:** CR-induced differential CH methylation is enriched in CG-rich genomic regions. **A.** Enrichment
725 of diet-dmCHs in gene-centric regions, only significant enrichments are shown ($p < 0.05$, hypergeometric
726 test). Diet-dmCHs were found to be enriched in CG islands and shores, promoters and gene bodies. **B.**
727 Enrichment of diet-dmCHs in gene-regulatory regions. Red indicates under-representation (log(odds
728 ratio) < 0 & p-value < 0.05, hypergeometric test), blue indicates over-representation (log(odds ratio) > 0
729 & p-value < 0.05, hypergeometric test) and white show no significance **C.** Pathway analysis of genes
730 containing >2 significant diet-dmCHs. Top enrichment pathways are shown (FDR adjusted p-values <
731 0.01). Circle size indicates the ratio of genes in pathway containing diet-dmCHs, color indicates p-values.
732 **D.** Overlap between pathways enriched for diet-dmCHs and diet-dmCGs.

733 **Figure 6:** Diet induced differential methylation involved in auto-regulation of DNA regulatory enzymes.
734 **A.** Calorie-restriction induces hypermethylation of CGs (red) and CHs (green) in the promoter regions of

735 TET3 **B.** mRNA expression of TET3 decreases with diet but not age (n=7-8/group, $F_{(2,20)} = 11.1$, ** $p <$

736 0.001, One-way ANOVA with Benjamini-Hochberg correction). **C.** Calorie-restriction induces

737 hypermethylation of CGs (red) and CHs (green) in the promoter regions of DNMT1. **D.** mRNA expression

738 of DNMT1 using an assay inclusive of all known DNMT1 isoforms show no significant differences with

739 age or diet (n=7-8/group, $F_{(2,20)} = 0.535$, $p > 0.05$, One-way ANOVA with Benjamini-Hochberg correction).

740 **E.** Isoform specific assays were used to assess expression of DNMT1 show significant decrease in DNMT1

741 expression with age and diet in isoforms utilizing exon 1 but no difference in expression when

742 examining isoforms using the alternative exon 1 (n=7-8/group, $F_{(2,19)} = 13.42$, * $p < 0.05$, **$p < 0.001$,

743 One-way ANOVA). **F.** mRNA expression of DNMT3a1 decreases with diet and age. TET1 expression did

744 not change in any condition and TET2 expression decreased with diet but not age (n=7-8/group,

745 DNMT3a1 $F_{(2,19)} = 18.59$, $Tet2_{(2,19)}$ $F = 10.6$, TET1 $F_{(2,20)} = 3.2$, *$p < 0.05$, **$p < 0.001$, One-way ANOVA

746 with Benjamini-Hochberg correction).

Figure 1

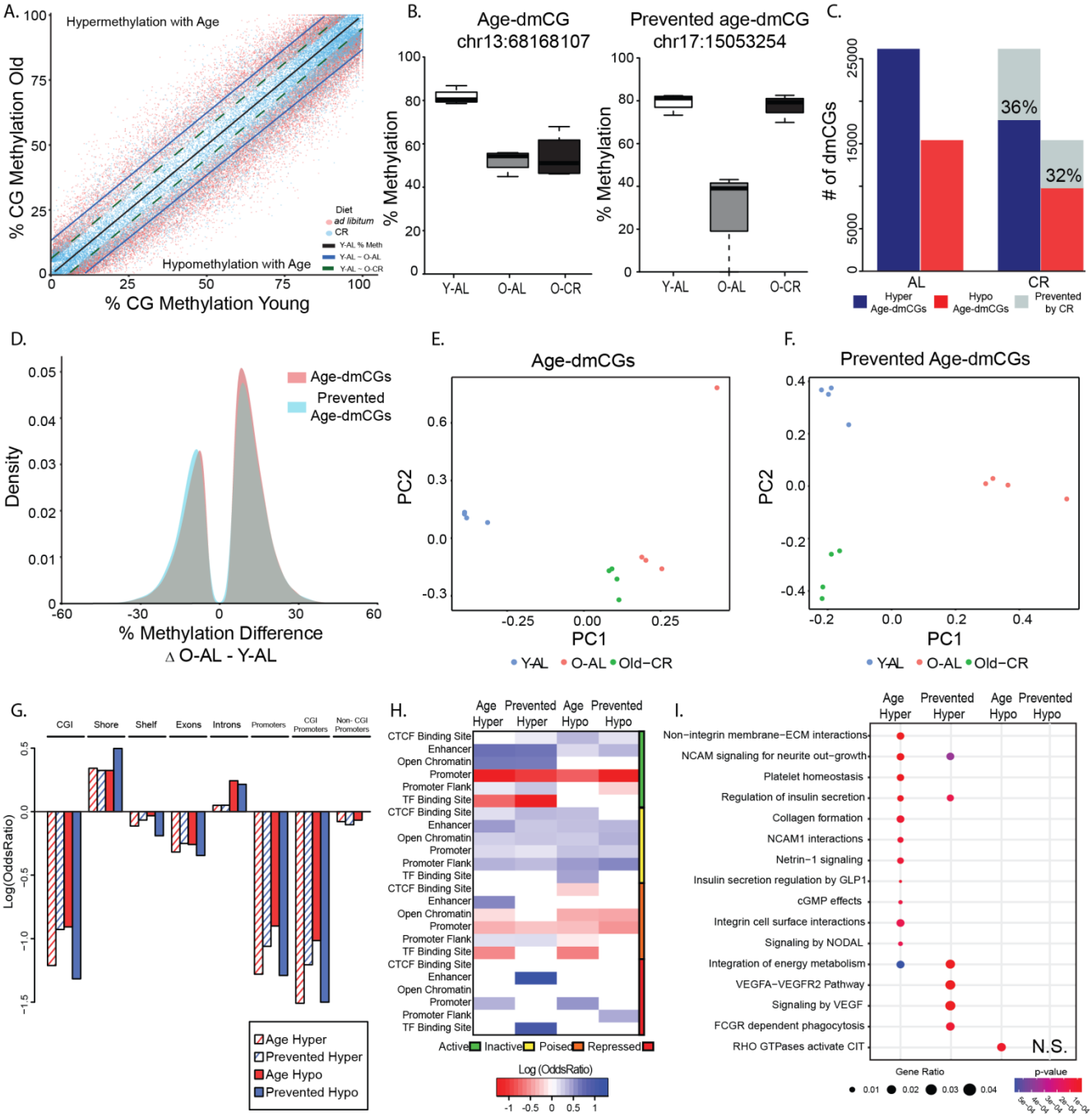
A.
Hypermethylation with Age
Hypomethylation with Age
% CG Methylation Old
% CG Methylation Young
Diet
ad libitum
CR
Y-AL % Meth
Y-AL ~ O-AL
Y-AL ~ O-CR
B.
Age-dmCG
chr13:68168107
Prevented age-dmCG
chr17:15053254
% Methylation
Y-AL
O-AL
O-CR
C.
# of dmCGs
36%
32%
AL
CR
Hyper Age-dmCGs
Hypo Age-dmCGs
Prevented by CR
D.
Age-dmCGs
Prevented Age-dmCGs
Density
% Methylation Difference
Δ O-AL - Y-AL
E.
Age-dmCGs
PC1
PC2
Y-AL
O-AL
Old-CR
F.
Prevented Age-dmCGs
PC1
PC2
Y-AL
O-AL
Old-CR
G.
CGI
Shore
Shelf
Exons
Introns
Promoters
CGI Promoters
Non- CGI Promoters
Log(OddsRatio)
Age Hyper
Prevented Hyper
Age Hypo
Prevented Hypo
H.
Age Hyper
Prevented Hyper
Age Hypo
Prevented Hypo
CTCF Binding Site
Enhancer
Open Chromatin
Promoter
Promoter Flank
TF Binding Site
Active
Inactive
Poised
Repressed
Log (OddsRatio)
I.
Age Hyper
Prevented Hyper
Age Hypo
Prevented Hypo
Non-integrin membrane-ECM interactions
NCAM signaling for neurite out-growth
Platelet homeostasis
Regulation of insulin secretion
Collagen formation
NCAM1 interactions
Netrin-1 signaling
Insulin secretion regulation by GLP1
cGMP effects
Integrin cell surface interactions
Signaling by NODAL
Integration of energy metabolism
VEGFA-VEGFR2 Pathway
Signaling by VEGF
FCGR dependent phagocytosis
RHO GTPases activate CIT
N.S.
Gene Ratio
p-value

Figure 2

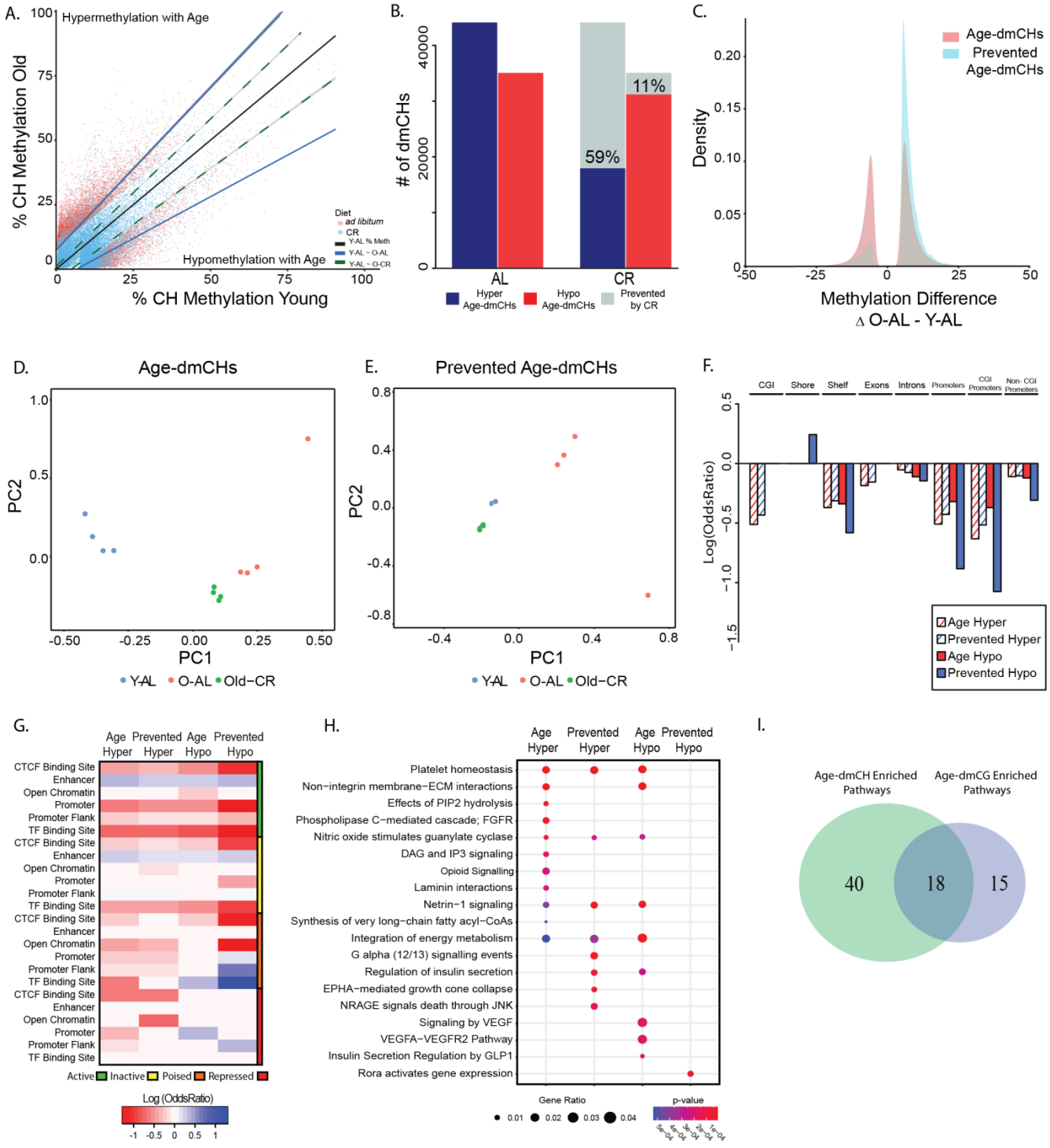
A.
Hypermethylation with Age
Hypomethylation with Age
% CH Methylation Old
% CH Methylation Young
Diet
ad libitum
CR
Y-AL % Meth
Y-AL ~ O-AL
Y-AL ~ O-CR
B.
# of dmCHs
59%
11%
AL
CR
Hyper Age-dmCHs
Hypo Age-dmCHs
Prevented by CR
C.
Age-dmCHs
Prevented Age-dmCHs
Density
Methylation Difference
Δ O-AL - Y-AL
D.
Age-dmCHs
PC1
PC2
Y-AL
O-AL
Old-CR
E.
Prevented Age-dmCHs
PC1
PC2
Y-AL
O-AL
Old-CR
F.
CGI
Shore
Shelf
Exons
Introns
Promoters
CGI Promoters
Non- CGI Promoters
Log(OddsRatio)
Age Hyper
Prevented Hyper
Age Hypo
Prevented Hypo
G.
Age Hyper
Prevented Hyper
Age Hypo
Prevented Hypo
CTCF Binding Site
Enhancer
Open Chromatin
Promoter
Promoter Flank
TF Binding Site
Active
Inactive
Poised
Repressed
Log (OddsRatio)
H.
Platelet homeostasis
Non−integrin membrane−ECM interactions
Effects of PIP2 hydrolysis
Phospholipase C−mediated cascade; FGFR
Nitric oxide stimulates guanylate cyclase
DAG and IP3 signaling
Opioid Signalling
Laminin interactions
Netrin−1 signaling
Synthesis of very long−chain fatty acyl−CoAs
Integration of energy metabolism
G alpha (12/13) signalling events
Regulation of insulin secretion
EPHA−mediated growth cone collapse
NRAGE signals death through JNK
Signaling by VEGF
VEGFA−VEGFR2 Pathway
Insulin Secretion Regulation by GLP1
Rora activates gene expression
Gene Ratio
p-value
I.
Age-dmCH Enriched Pathways
Age-dmCG Enriched Pathways
40
18
15

Figure 3

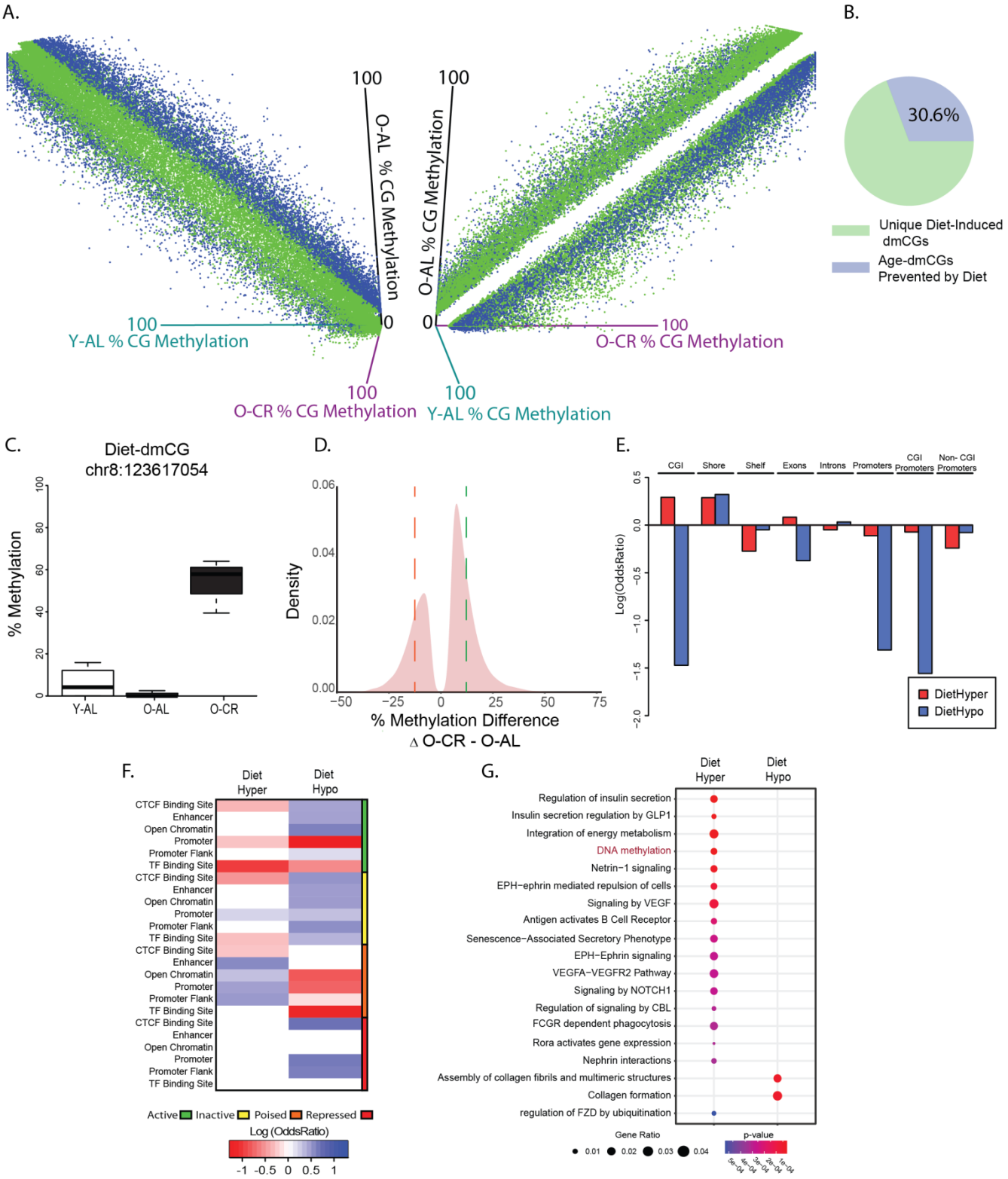
A.
100
O-AL % CG Methylation
100
Y-AL % CG Methylation
100
O-CR % CG Methylation
100
O-AL % CG Methylation
0
100
O-CR % CG Methylation
100
Y-AL % CG Methylation
B.
30.6%
Unique Diet-Induced dmCGs
Age-dmCGs Prevented by Diet
C.
Diet-dmCG
chr8:123617054
% Methylation
Y-AL
O-AL
O-CR
D.
Density
% Methylation Difference
Δ O-CR - O-AL
E.
CGI
Shore
Shelf
Exons
Introns
Promoters
CGI Promoters
Non- CGI Promoters
Log(OddsRatio)
DietHyper
DietHypo
F.
Diet Hyper
Diet Hypo
CTCF Binding Site
Enhancer
Open Chromatin
Promoter
Promoter Flank
TF Binding Site
Active
Inactive
Poised
Repressed
Log (OddsRatio)
G.
Diet Hyper
Diet Hypo
Regulation of insulin secretion
Insulin secretion regulation by GLP1
Integration of energy metabolism
DNA methylation
Netrin−1 signaling
EPH−ephrin mediated repulsion of cells
Signaling by VEGF
Antigen activates B Cell Receptor
Senescence−Associated Secretory Phenotype
EPH−Ephrin signaling
VEGFA−VEGFR2 Pathway
Signaling by NOTCH1
Regulation of signaling by CBL
FCGR dependent phagocytosis
Rora activates gene expression
Nephrin interactions
Assembly of collagen fibrils and multimeric structures
Collagen formation
regulation of FZD by ubiquitination
Gene Ratio
p-value

Figure 4

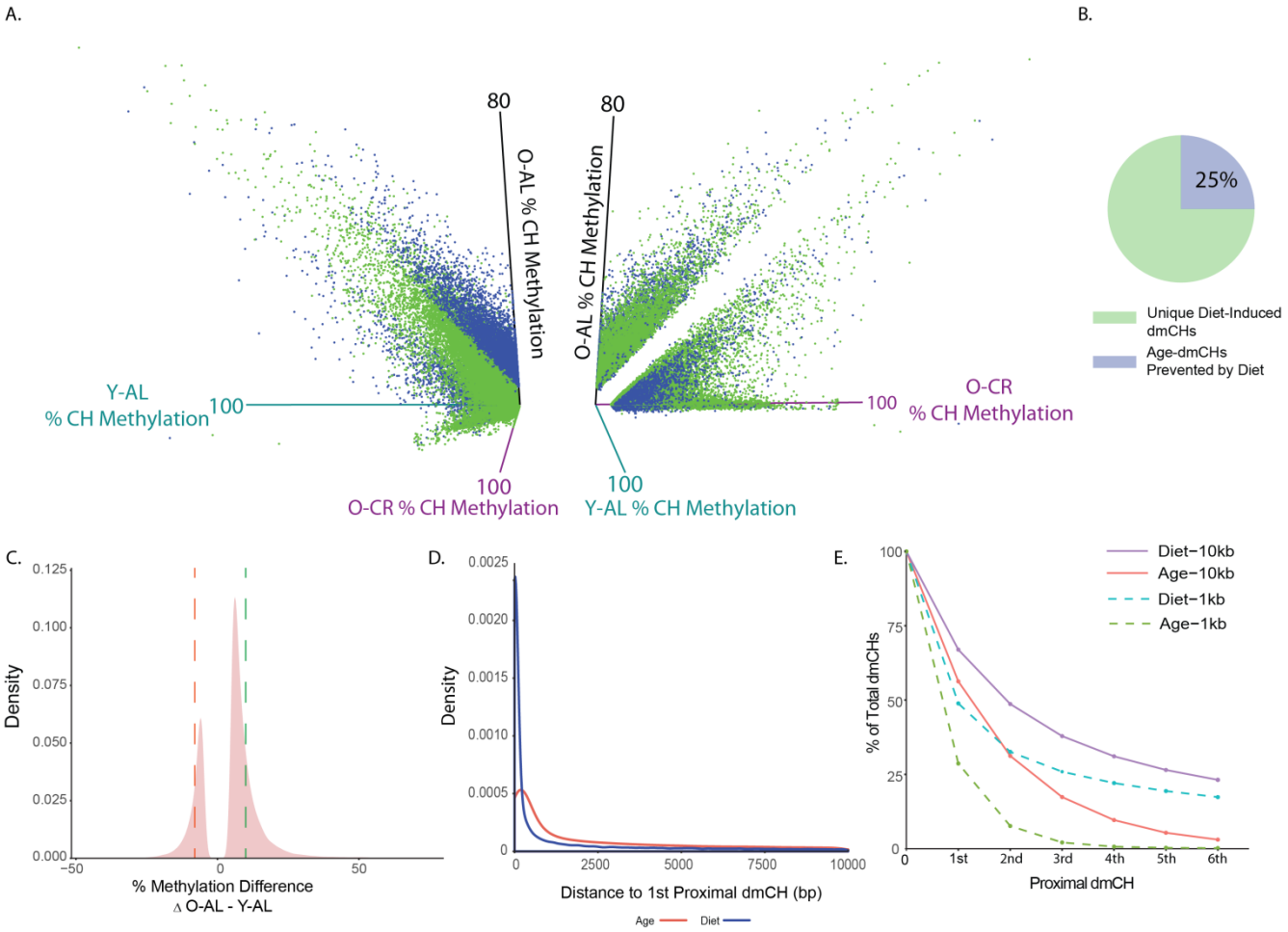
A.
B.
80
80
O-AL % CH Methylation
O-AL % CH Methylation
Y-AL
% CH Methylation
100
100
O-CR
% CH Methylation
100
O-CR % CH Methylation
100
Y-AL % CH Methylation
25%
Unique Diet-Induced dmCHs
Age-dmCHs Prevented by Diet
C.
Density
% Methylation Difference
Δ O-AL - Y-AL
D.
Density
Distance to 1st Proximal dmCH (bp)
Age
Diet
E.
% of Total dmCHs
Proximal dmCH
Diet−10kb
Age−10kb
Diet−1kb
Age−1kb

Figure 5

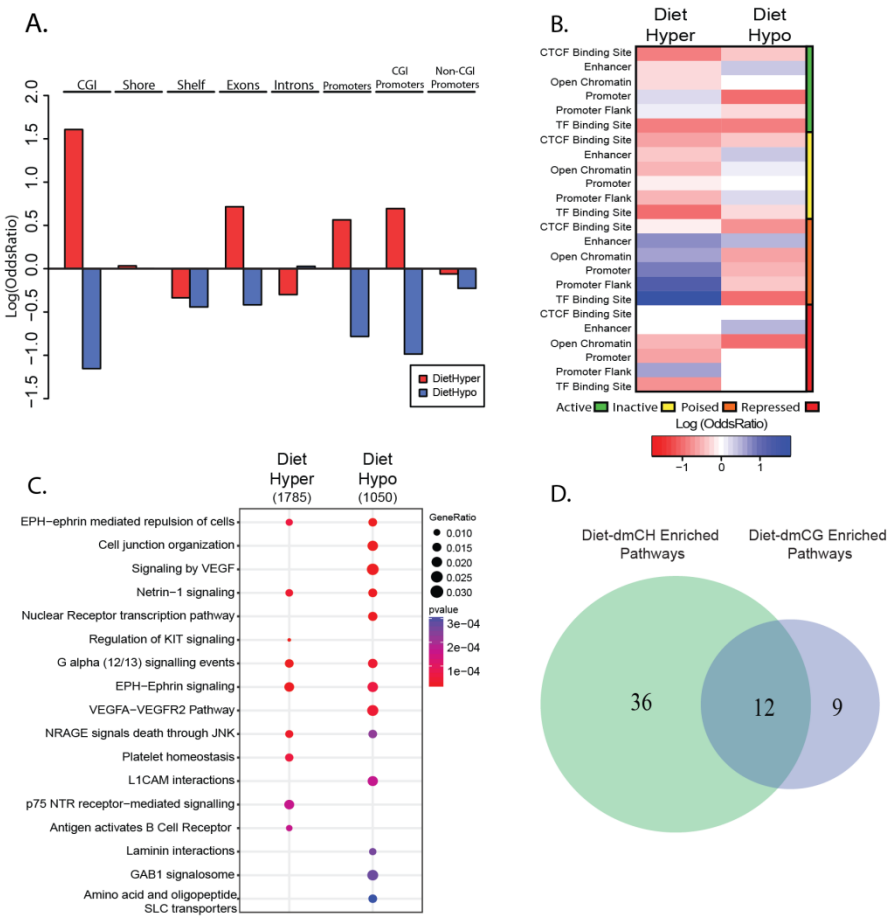
A.
CGI
Shore
Shelf
Exons
Introns
Promoters
CGI Promoters
Non-CGI Promoters
Log(OddsRatio)
2.0
1.5
1.0
0.5
0.0
−0.5
−1.0
−1.5
DietHyper
DietHypo
B.
Diet Hyper
Diet Hypo
CTCF Binding Site
Enhancer
Open Chromatin
Promoter
Promoter Flank
TF Binding Site
Active
Inactive
Poised
Repressed
Log (OddsRatio)
−1
0
1
C.
Diet Hyper (1785)
Diet Hypo (1050)
EPH−ephrin mediated repulsion of cells
Cell junction organization
Signaling by VEGF
Netrin−1 signaling
Nuclear Receptor transcription pathway
Regulation of KIT signaling
G alpha (12/13) signalling events
EPH−Ephrin signaling
VEGFA−VEGFR2 Pathway
NRAGE signals death through JNK
Platelet homeostasis
L1CAM interactions
p75 NTR receptor−mediated signalling
Antigen activates B Cell Receptor
Laminin interactions
GAB1 signalosome
Amino acid and oligopeptide, SLC transporters
GeneRatio
0.010
0.015
0.020
0.025
0.030
pvalue
3e−04
2e−04
1e−04
D.
Diet-dmCH Enriched Pathways
Diet-dmCG Enriched Pathways
36
12
9

Figure 6

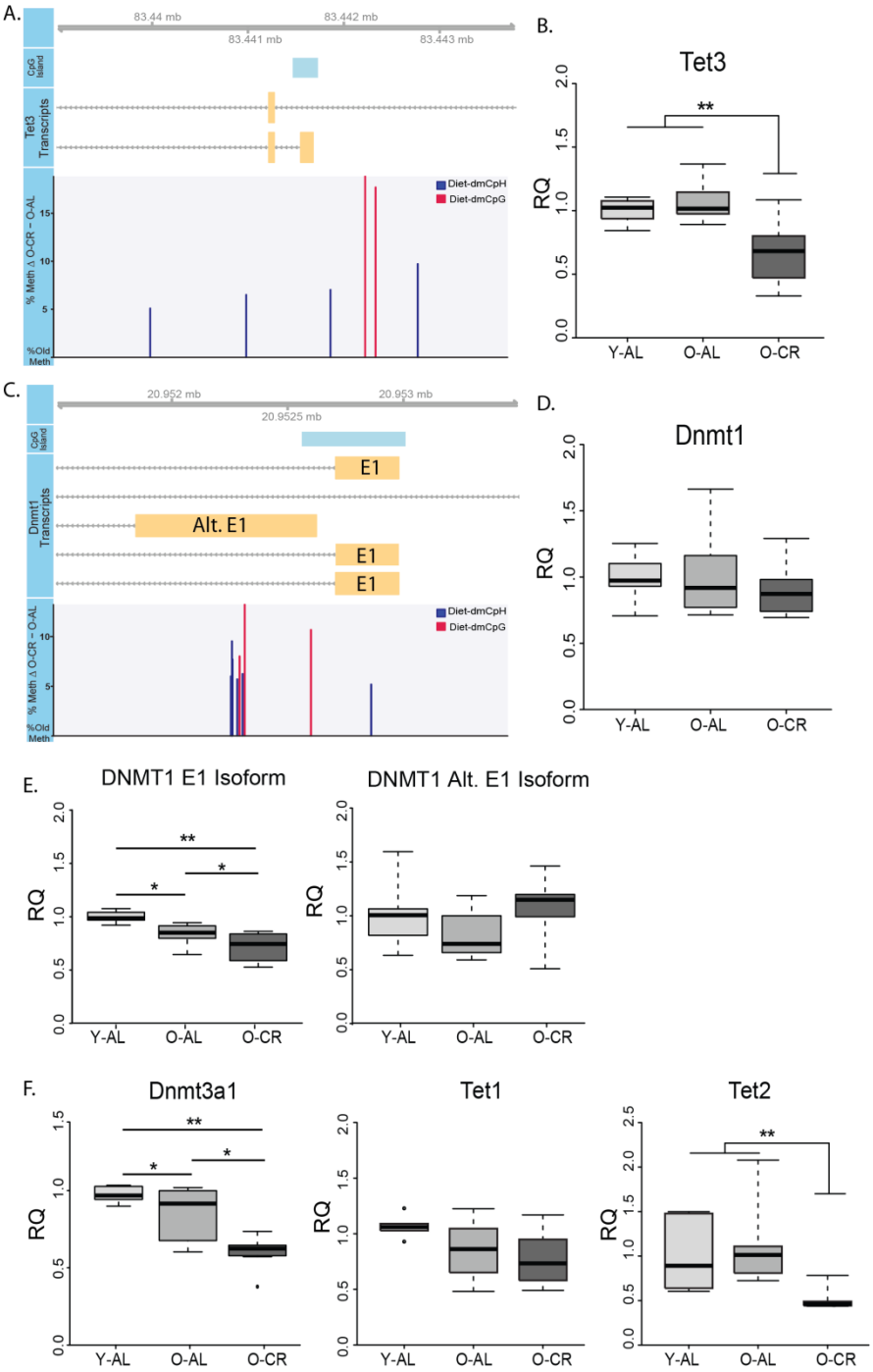
A.
83.44 mb
83.442 mb
83.441 mb
83.443 mb
CpG Island
Tet3 Transcripts
Diet-dmCpH
Diet-dmCpG
% Meth Δ O-CR – O-AL
%Old Meth
B.
Tet3
RQ
Y-AL
O-AL
O-CR
C.
20.952 mb
20.953 mb
20.9525 mb
CpG Island
Dnmt1 Transcripts
E1
Alt. E1
E1
E1
Diet-dmCpH
Diet-dmCpG
% Meth Δ O-CR – O-AL
%Old Meth
D.
Dnmt1
RQ
Y-AL
O-AL
O-CR
E.
DNMT1 E1 Isoform
DNMT1 Alt. E1 Isoform
RQ
Y-AL
O-AL
O-CR
F.
Dnmt3a1
Tet1
Tet2
RQ
Y-AL
O-AL
O-CR